Heat Mass Transfer (2005) 41: 387–398
DOI 10.1007/s00231-004-0537-1

ORIGINAL

H. S. Takhar · A. J. Chamkha · G. Nath

Unsteady mixed convection on the stagnation-point flow adjacent to a vertical plate with a magnetic field

Received: 25 July 2003 / Published online: 10 August 2004

Abstract An analysis is performed to study the unsteady combined forced and free convection flow (mixed convection flow) of a viscous incompressible electrically conducting fluid in the vicinity of an axisymmetric stagnation point adjacent to a heated vertical surface. The unsteadiness in the flow and temperature fields is due to the free stream velocity, which varies arbitrarily with time. Both constant wall temperature and constant heat flux conditions are considered in this analysis. By using suitable transformations, the Navier–Stokes and energy equations with four independent variables (x, y, z, t) are reduced to a system of partial differential equations with two independent variables (η, τ). These transformations also uncouple the momentum and energy equations resulting in a primary axisymmetric flow, in an energy equation dependent on the primary flow and in a buoyancy-induced secondary flow dependent on both primary flow and energy. The resulting system of partial differential equations has been solved numerically by using both implicit finite-difference scheme and differential-difference method. An interesting result is that for a decelerating free stream velocity, flow reversal occurs in the primary flow after certain instant of time and the magnetic field delays or prevents the flow reversal. The surface heat transfer and the surface shear stress in the primary flow increase with the magnetic field, but the surface shear stress in the buoyancy-induced secondary flow decreases. Further the heat transfer increases with the Prandtl number, but the surface shear stress in the secondary flow decreases.

H. S. Takhar (✉)
Department of Engineering,
Manchester Metropolitan University,
Manchester, M1 5GD, UK
E-mail: H.S.Takhar@mmu.ac.uk

A. J. Chamkha
Department of Mechanical Engineering,
Kuwait University, P.O. Box 5969,
Safat, 13060, Kuwait

G. Nath
Department of Mathematics,
Indian Institute of Science,
Bangalore, 560012, India

List of symbols

C_f	specific heat of the fluid
C_{fx}	local skin friction coefficient
f	dimensionless stream function
g	acceleration due to gravity
Gr	Grashof number
Gr_x	local Grashof number
M	magnetic parameter
Nu_x	local Nusselt number
Pr	Prandtl number
Re_m	magnetic Reynolds number
x, y, z	Cartesian co-ordinates
T	temperature
u, v, w	velocity components along radial and axial directions
β	volumetric coefficient of thermal expansion
η, ξ	transformed co-ordinates
θ	dimensionless temperature
μ	coefficient of viscosity
ν	kinematic viscosity
ρ_f	density of the fluid
Ψ	dimensional stream function

Subscripts

w, ∞	conditions at the wall and in the ambient fluid

Superscript

′	derivative with respect to η

1 Introduction

The combined forced and free convection flow (mixed convective flow) is encountered in several industrial

and technical applications, which include nuclear reactors cooled during emergency shutdown, electronic devices cooled by fans, heat exchangers placed in a low-velocity environment, solar central receivers expand to wind current. Sparrow et al. [1] were the first to investigate the effect of buoyancy forces on the forced convection flow over a vertical flat plate and obtained the similarity solution when both the wall temperature and external flow vary with the streamwise distance from the leading edge of the plate in a particular manner. Sparrow and Gregg [2] further obtained the nonsimilar solution of the mixed convection flow over a vertical plate by using a series solution method. Merkin [3] investigated the mixed convection flow over an isothermal vertical plate when the buoyancy forces aid or oppose the forced convection flow. Two series solutions were obtained, one of which is valid near the leading edge and the other is valid asymptotically. In the region where the series solutions are not valid, the equations were solved numerically. Oosthuizen and Hart [4] studied the mixed convection flow over a heated vertical plate by using the finite-difference method. Mucoglu and Chen [5] considered the mixed convection flow over an inclined surface for both constant wall temperature and constant heat flux cases. The governing boundary layer equations were solved by using an implicit finite-difference scheme developed by Keller [6] as well as by local nonsimilarity method [7]. The similarity solutions for the mixed convection on a vertical plate for constant heat flux conditions on the wall were obtained by Merkin and Mahmood [8]. The influence of the inclination angle and the Prandtl number on the mixed convection flow over an inclined plate for both constant wall temperature and constant wall heat flux conditions was considered by Wickern [9, 10] and the governing boundary layer equations were solved by employing an implicit finite-difference scheme. Watanabe [11] studied the effects of surface suction/injection on the mixed convection flow over the vertical surface for the constant wall temperature (CWT) case and the governing partial differential equations were solved by the differential-difference method [12]. Ramachandran et al. [13] analyzed the mixed convection in 2D stagnation flow adjacent to a vertical surface for both cases of an arbitrary wall temperature and arbitrary surface heat flux variations and obtained similarity solutions. The resulting ordinary differential equations were solved by the fourth-order Runge–Kutta integration scheme along with the Nachtsheim–Swigert shooting technique [14]. The mixed convection flow at a 2D stagnation point on a heated horizontal boundary was studied by Amin and Riley [15]. The forced convection is a stagnation point flow and the free convection part is due to a pressure gradient that is induced by the temperature variations along the boundary.

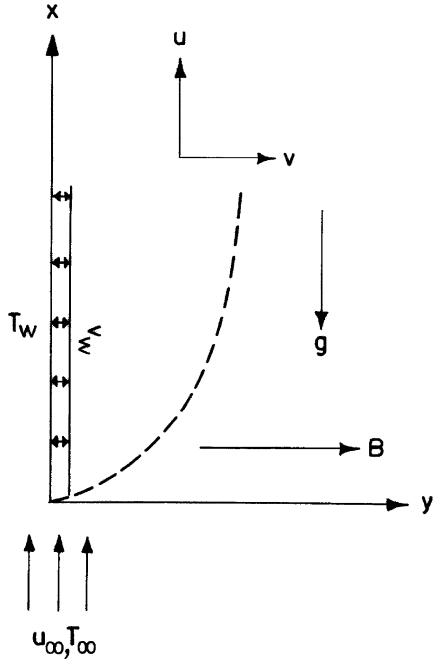

Fig. 1 Physical Model

The studies mentioned above dealt with the steady flows, but many problems of practical interest may be unsteady. The unsteadiness is due to the change in the free stream velocity and (or) wall temperature (heat flux) or due to both. Brown and Riley [16] studied the temporal development of the free convection flow past a suddenly heated semi-infinite vertical plate. The unsteadiness in the flow field was induced by the step-change in the wall temperature (heat flux) and (or) in the free stream velocity. They found that in the initial stage in the flow is governed by one-dimensional flow model and the early stage of the departure from this is described by a local solution. On the other hand, Ingham [17] reconsidered the problem of Brown and Riley [16] where the wall temperature was suddenly raised from the ambient temperature T_∞ to T_w ($T_w = T_\infty + A_x{}^m$, where A and m are positive constants and x is the distance measured from the leading edge of the plate) and obtained the solutions of the governing equations by using both numerical and asymptotic methods. Sammakia et al [18] and Harris et al. [19] have, respectively, studied the transient mixed and free convection flows past a heated vertical flat surface and the governing partial differential equations were solved by the finite-difference scheme. Seshadri et al. [20] investigated the unsteady mixed convection in the stagnation flow adjacent to a heated vertical flat plate. The unsteadiness in the problem was introduced by the impulsive motion of the free stream velocity and by sudden increase in the wall temperature (heat flux). The boundary layer equations were solved by using an implicit finite-difference scheme starting from the initial steady state to the final steady state. Wang [21] studied the steady natural convection in the axisymmetric stagnation-point flow on a heated vertical surface and obtained the similarity solution.

It may be remarked that Rott and Lewellen [22], Chawla and Verma [23] and Thacker et al. [24] have shown that the axisymmetric character in rotating flows is destroyed when translocational velocity or buoyancy force is imposed on the flow field. The buoyancy force in the free or mixed convection flow in the axisymmetric stagnation-point flow also destroys the axisymmetric nature of the flow [21]. Consequently, the flow field depends on all the three space variables (x, y, z).

The aim of this analysis is to study the unsteady mixed convection in the axisymmetric stagnation-point flow adjacent to a heated vertical surface in the presence of a magnetic field. Both constant wall temperature and constant heat flux conditions are considered. By using suitable transformations the Navier–Stokes equations and the energy equation which are represented by a system of partial differential equations with four independent variables (x, y, z, t) governing the flow can be reduced to a system of partial differential equations with two independent variables (η, τ). Also these transformations uncouple the momentum and energy equations in a primary axisymmetric flow in an energy equation dependent on the primary flow and in a buoyancy induced secondary flow dependent on both primary flow and energy. The resulting system of partial differential equations with two independent variables (η, τ) have been solved by using an implicit finite difference scheme similar to that of Blottner [25] and also by the differential-difference method [12]. The steady-state results have been compared with those of Sparrow et al. [26]. The present analysis may be regarded as an extension of the work of Wang [21] to include the effects of unsteadiness, free stream velocity and the magnetic field. Also it may be considered as the axisymmetric and magnetic counterpart of the problem considered in [20]. For decelerating free stream velocity, the flow reversal occurs after certain instant of time and the magnetic field delays or prevents this reversal of flow. The magnetic field also retards the growth of the buoyancy-induced secondary flow. Hence the present study could be useful in nuclear engineering where the flow reversal could be delayed or prevented and the secondary flow could be controlled by the application of the magnetic field.

2 Formulation and analysis

Let us consider that a fluid stream impinges on a wall at right angles to it and flows away radially in all directions. Such a flow occurs in the vicinity of a stagnation point of a body of revolution in a flow parallel to the axis. We use the Cartesian coordinate system (x, y, z), shown in Fig. 1. We assume that the wall is at $z=0$, the stagnation point is at the origin and the flow is in the direction of the negative z-axis. The buoyancy force acts along the negative x-axis. We consider the unsteady, incompressible mixed convection of a viscous electrically conducting fluid in an axisymmetric stagnation flow near a vertical flat plate. The unsteadiness in the flow field is introduced by the time-dependent free stream velocity. Let U, V and W are the velocity components in the x, y and z directions in the potential flow and u, v and w are the corresponding velocity components in the viscous flow. The surface is kept at a constant temperature or at a constant heat flux. The wall temperature T_w or the heat flux at the surface q_w and free stream temperature T_∞ are constants with $T_w > T_\infty$. The density variations are neglected except where necessary for driving the buoyancy force. The magnetic field B is applied normal to the surface (i.e., in the z-direction). It is assumed that the magnetic Reynolds number $\mathrm{Re_m} = \mu_0 \sigma V^* L << 1$, where μ_0 is the magnetic permeability, σ is the electrical conductivity, and V^* and L are the characteristic velocity and length, respectively. Under this assumption, it is possible to neglect the induced magnetic field in comparison to the applied magnetic field. The vertical plate is assumed to be electrically non-conducting and the fluid is taken to be electrically conducting. The viscous dissipation and Ohmic heating terms are not included in the energy equation since they are, generally, small in the vicinity of the stagnation point. Under the above assumptions, the Navier–Stokes equations and the energy equation governing the unsteady flow in the vicinity of an axisymmetric stagnation flow adjacent to a vertical plate can be expressed as [13, 21, 24, 27].

$$u_x + v_y + w_z = 0, \tag{1}$$

$$u_t + uu_x + vu_y + wu_z = -\rho^{-1} p_x + \nu \nabla^2 u + g\beta(T - T_\infty) - \rho^{-1} \rho B^2 u, \tag{2}$$

$$v_t + uv_x + vv_y + wv_z = -\rho^{-1} p_y + \nu \nabla^2 v + \rho^{-1} \sigma B^2 v, \tag{3}$$

$$w_t + uw_x + vw_y + ww_z = -\rho^{-1} p_z + \nu \nabla^2 w, \tag{4}$$

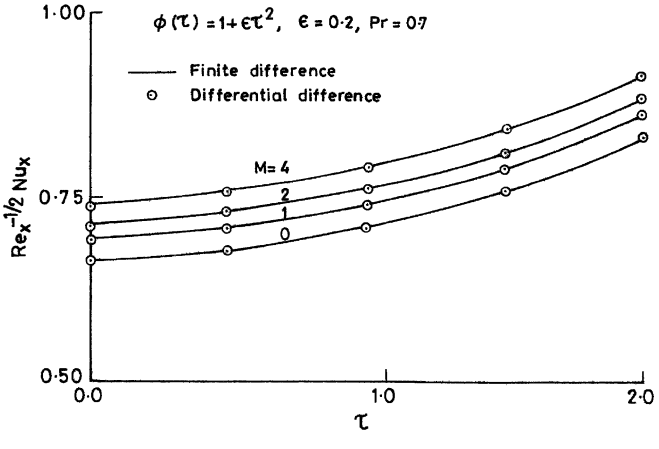

Fig. 2 Comparison of the Nusselt number $\mathrm{Re_x^{-1/2}\ Nu_x}$, for the CWT case, obtained by finite-difference and different-difference methods

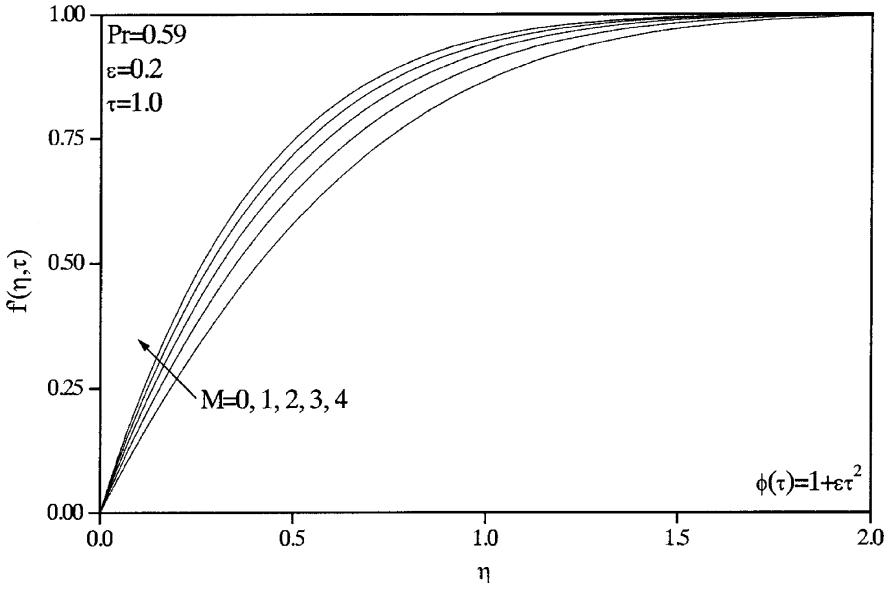

Fig. 3 Effect of magnetic parameter M on the velocity profiles in the primary flow, $f'(\eta, \tau)$

$$T_t = uT_x + vT_y + wT_z = \alpha\nabla^2 T, \tag{5}$$

where

$$\nabla^2 = \frac{\partial^2}{\partial x^2} + \frac{\partial^2}{\partial y^2} + \frac{\partial^2}{\partial z^2}. \tag{6}$$

The initial conditions (i.e., conditions at time $t=0$) are given by

$$u = u_i, \quad v = v_i, \quad w = w_i, \quad p = p_i, \quad T = T_i. \tag{7}$$

The boundary conditions can be expressed as,

$$u = v = w = 0, \quad p = p_0, \quad T = T_w \quad \text{at } z = 0,\ x \geq 0,\ y \geq 0,$$

$$u \to U, \quad v \to V, \quad w \to W, \quad T \to T_\infty \quad \text{as } z \to \infty,\ x \geq 0,\ y \geq 0,$$

$$u = U,\ v = V,\ w = W,\ T = T_\infty \ \text{at } x = 0,\ y > 0,\ z > 0,$$
$$u = U,\ v = V,\ w = W,\ T = T_\infty \ \text{at } y = 0,\ x > 0,\ z > 0. \tag{8}$$

Here p is the static pressure, ρ and ν are the density and kinematic viscosity, respectively, p_0 is the stagnation pressure, T is the temperature, the subscript i denotes initial conditions, the subscripts w and ∞ denote conditions at the wall and in the free stream, respectively, and the subscripts t, x, y and z denote derivatives with respect to t, x, y, z, respectively. α is the thermal diffu-

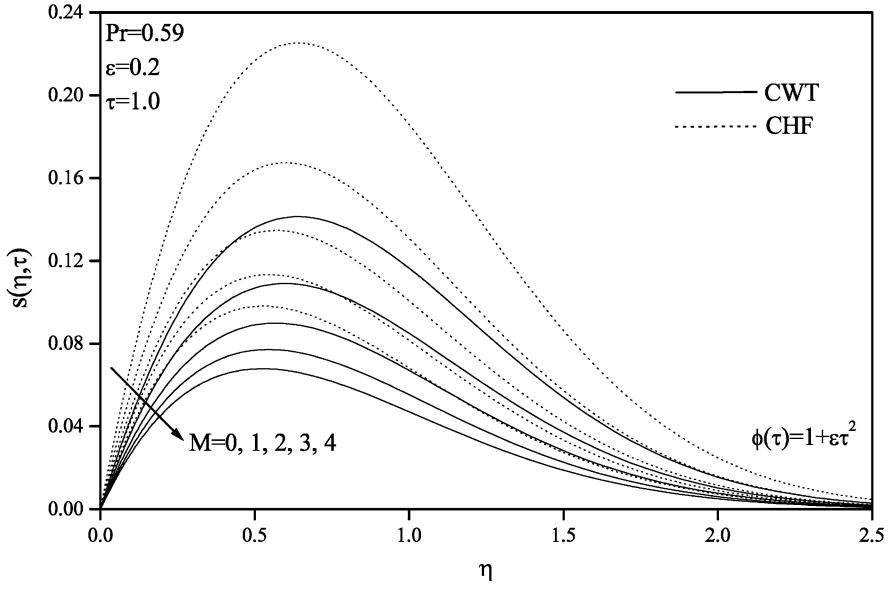

Fig. 4 Effect of magnetic parameter M on the velocity profiles in the secondary flow, $s(\eta, \tau)$

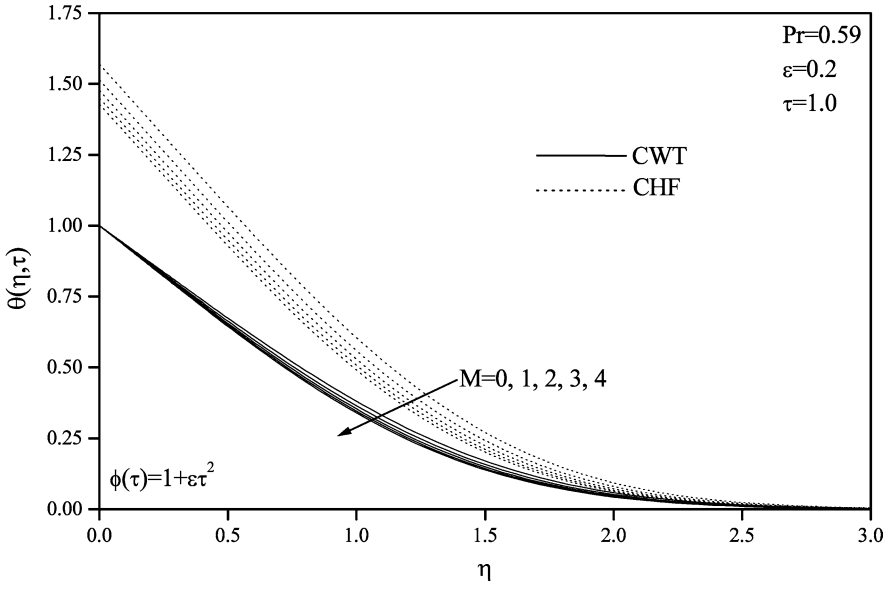

Fig. 5 Effect of magnetic parameter M on the temperature profiles, θ (η, τ)

sivity, g is the magnitude of gravitational acceleration and β is the volumetric coefficient of thermal expansion.

Equations 1, 2, 3, 4, 5 are partial differential equations with four independent variables (t, x, y, z). However, it is possible to reduce Eqs. 1, 2, 3, 4, 5 to partial differential equations with two independent variables (η, τ) if the potential velocity components in x and y-directions are of the form

$$\begin{aligned} U &= ax\,\phi(\tau), \quad V = ay\,\phi(\tau), \quad \tau = at, \\ a &= \left(\tfrac{\partial U}{\partial x}\right)_{\tau=0} = \left(\tfrac{\partial V}{\partial y}\right)_{\tau=0} = 0, \quad \phi(0) = 1. \end{aligned} \tag{9}$$

Then from the continuity equation

$$W = -2a\,\phi(\tau)z. \tag{10}$$

Using the unsteady Bernoulli equation, the pressure p is given by

$$p_0 - p = 2^{-1}\rho a^2\left[\left(\phi^2 + M\phi + \frac{\partial\phi}{\partial\tau}\right)(x^2+y^2) + 2\left(2\phi^2 - \frac{\mathrm{d}\phi}{\mathrm{d}\tau}\right)z^2\right], \tag{11}$$

where

$$M = \frac{\sigma B^2}{\rho \mathrm{a}}. \tag{12}$$

Now, we apply the following transformations

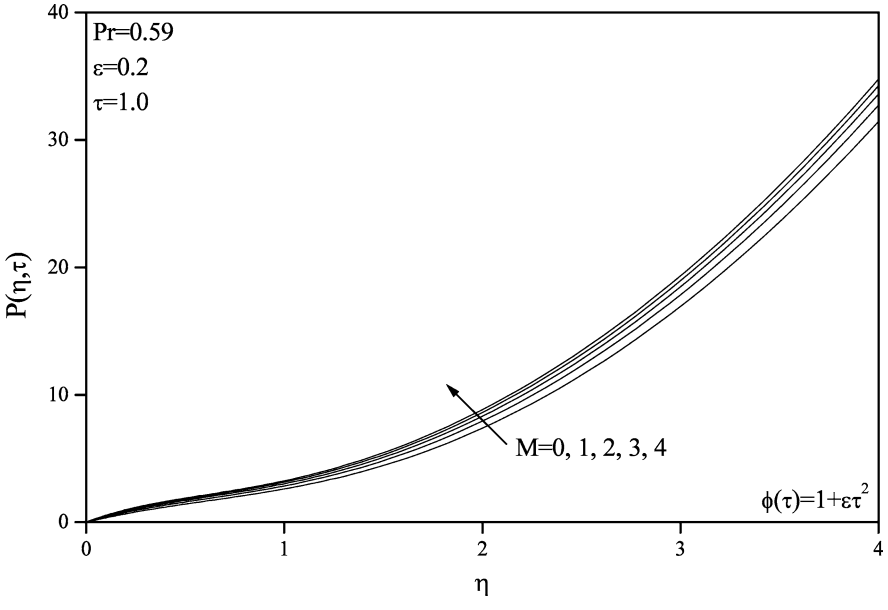

Fig. 6 Effect of magnetic parameter M on the pressure profiles $P(\eta, \tau)$

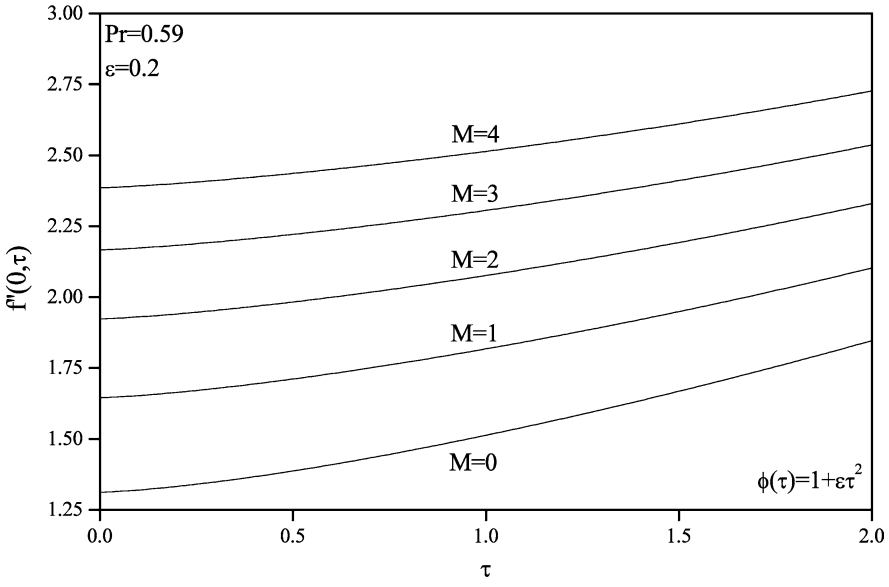

Fig. 7 Effect of magnetic parameter M on the surface shear stress in the primary flow, $f''(0, \tau)$, for accelerating flow

$$\eta=\left(\frac{a}{\nu}\right)^{1/2}z,\ \tau=at,\ u=ax\phi(\tau)f'(\eta,\tau)+g\beta(T-T_\infty)a^{-1}s(\eta,\tau),$$
$$v=ay\phi(\tau)f'(\eta,\tau),\ w=-2(a\nu)^{1/2}\phi(\tau)f(\eta,\tau),$$
$$\theta(\eta,\tau)=\frac{T-T_\infty}{T_w-T_\infty},\ \mathrm{Pr}=\frac{\nu}{\alpha},$$
$$p_0-p=2^{-1}\rho a^2\left[\left(\phi^2+M\phi+\frac{\mathrm{d}\phi}{\mathrm{d}\tau}\right)(x^2+y^2)+2\left(\frac{\nu}{a}\right)P(\eta,\tau)\right], \tag{13}$$

to Eqs. 1, 2, 3, 4, 5 and we find that Eq. 1 is identically satisfied Eqs. 2, 3, 4, 5 reduce to

$$f'''+\phi(2ff''+1-f'^2)+M(1-f')+\phi^{-1}\frac{\mathrm{d}\phi}{\mathrm{d}\tau}(1-f')-\frac{\partial f'}{\partial\tau}=0 \tag{14}$$

$$s''+\phi(2fs'-f's)+\theta-Ms-\frac{\partial s}{\partial\tau}=0, \tag{15}$$

$$\mathrm{Pr}^{-1}\theta''+2\phi f\theta'-\frac{\partial\theta}{\partial\tau}=0, \tag{16}$$

$$P-2\phi(f'+\phi f^2)-2\frac{\partial}{\partial\tau}\int_0^\eta(\phi f)\partial\eta, \tag{17}$$

where the pressure P is written after integration which satisfies the boundary condition. The initial conditions are

$$f=f_i,\quad s=s_i,\quad \theta=\theta_I,\qquad \text{at } \tau=0, \tag{18}$$

and the boundary conditions are

$$f=f'=s=0,\quad \theta=1\qquad \text{at } \eta=0,$$
$$f'\to 1,\quad s\to 0,\quad \theta\to 0\quad \text{as } \eta\to\infty. \tag{19}$$

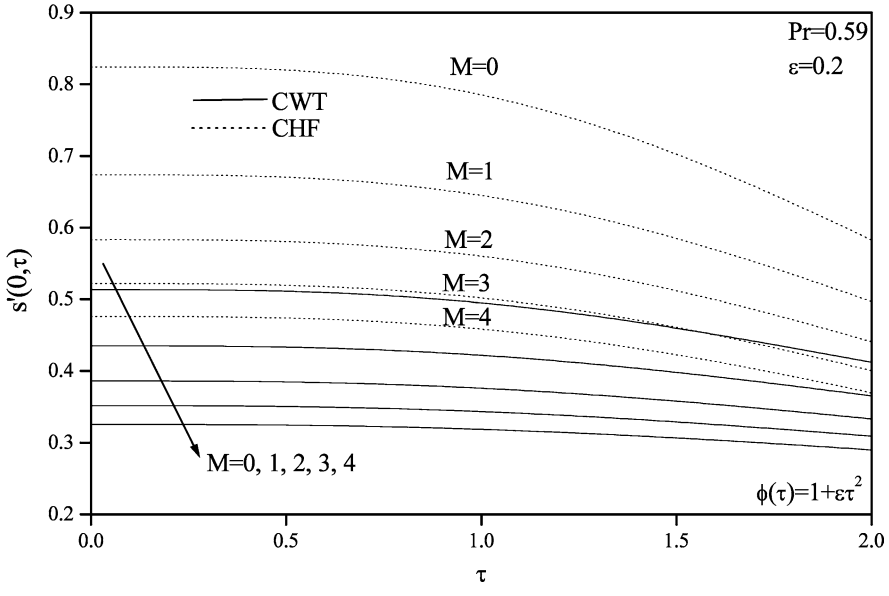

Fig. 8 Effect of magnetic parameter M on the surface shear stress in the secondary flow, $s'(0, \tau)$, for accelerating flow

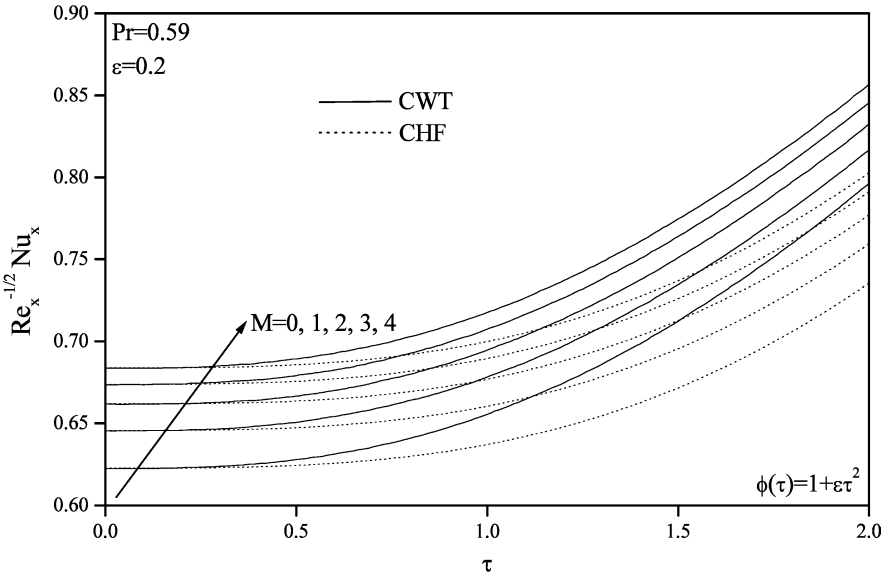

Fig. 9 Effect of magnetic parameter M on the Nusselt number, $Re_x^{-1/2}\,Nu_x$, for accelerating flow

The steady-state equations (i.e., at $\tau = 0$) are obtained from Eqs. 14, 15, 16, 17 by putting $\tau = \partial/\partial\tau = 0$, $\phi = 1$, $d\phi/d\tau = 0$ in them. These steady-state equations are

$$f''' + 2ff'' + 1 - f'^2 + M(1 - f') = 0, \tag{20}$$

$$s'' + 2fs' - f's + \theta - Ms = 0, \tag{21}$$

$$\mathrm{Pr}^{-1}\theta'' + 2f\theta' = 0, \tag{22}$$

$$P = 2(f' + f^2), \tag{23}$$

with boundary conditions,

$$\begin{aligned} f(0) = f'(0) = s(0) = \theta(0) = 0, \\ f'(\infty) - 1 = s(\infty) = \theta(\infty) = 0. \end{aligned} \tag{24}$$

Here η and τ are the transformed independent variables, f' and s are the dimensionless velocities in the primary and secondary flows, respectively (i.e., in x and y directions, respectively), P is the dimensionless pressure, a is the velocity gradient in the potential flow at time $\tau = 0$, $\varphi(\tau)$ is a function of time τ and is chosen such that both φ and $d\varphi/d\tau$ are continuous functions, Pr is the Prandtl number, M is the magnetic parameter and prime denotes derivative with respect to η.

It may be remarked that Eqs. 14, 15, 16, 17, 18, 19, 20, 21, 22, 23, 24 represent both Navier-Stokes equations as well as boundary layer equations in the axisymmetric stagnation point region. However, for boundary layer equations, Eqs. 17 and 23 are not required, because the pressure is assumed to be constant across the boundary layer. The steady-state Eqs. 20 and 22 are identical to those of Sparrow et al. [27].

The above equations are not only valid for the CWT case, but they are also valid for the constant heat flux (CHF) case except that

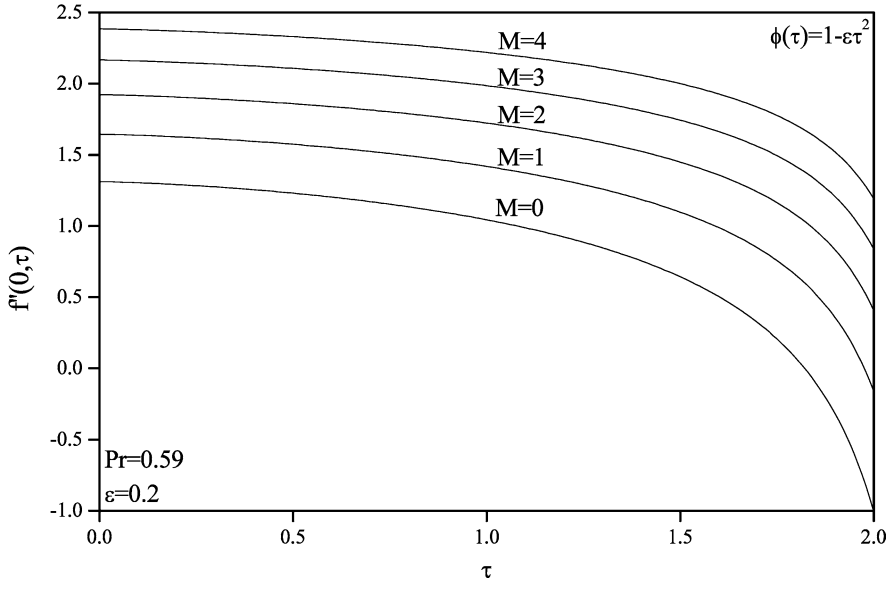

Fig. 10 Effect of magnetic parameter M on the surface shear stress in the primary flow, $f''(0, \tau)$, for decelerating flow

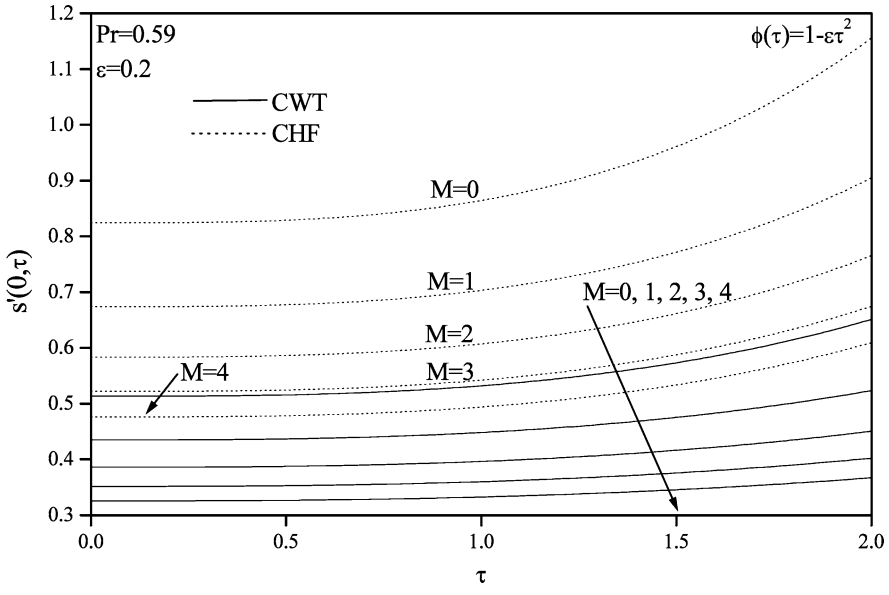

Fig. 11 Effect of magnetic parameter M on the surface shear stress in the secondary flow, $s'(0, \tau)$, for decelerating flow

$$\theta(\eta,\tau) = \left(\frac{a}{\nu}\right)^{1/2}\left(\frac{k}{q_{\mathrm{w}}}\right)(T - T_\infty), \tag{25}$$

$$u = ax\,\phi(\tau) f'(\eta,\tau) + \left[\left(\frac{\nu}{a}\right)^{1/2}\frac{g\beta\, q_{\mathrm{w}}}{ka}\right] s(\eta,\tau), \tag{26}$$

and the boundary conditions $\theta = 1$ at $\eta = 0$ in Eqs. 19 and 24 should be replaced by $\theta' = -1$ at $\eta = 0$.

The equations of physical interest are the Nusselt number and the skin friction coefficient. For the CWT case they are given by

$$\mathrm{Nu}_x = -x\frac{\left(\frac{\partial T}{\partial z}\right)_{z=0}}{T_{\mathrm{w}} - T_\infty} = -\mathrm{Re}_x^{1/2}\,\theta'(0,\tau), \tag{27}$$

$$C_{fx} = \frac{\mu\left(\frac{\partial u}{\partial z}\right)_{z=0}}{\rho U_0^2} = \mathrm{Re}_x^{1/2}[\phi\, f''(0,\tau) + \lambda\, s'(0,\tau)], \tag{28}$$

where

$$\mathrm{Re}_x = \frac{ax^2}{\nu},\quad U_0 = ax,\quad \lambda = \frac{\mathrm{Gr}_x}{\mathrm{Re}_x^2},\quad \mathrm{Gr}_x = g\beta\frac{(T_{\mathrm{w}} - T_\infty)x^3}{\nu^2}. \tag{29}$$

The corresponding expressions for the CHF case are

$$\mathrm{Nu}_x = \frac{\mathrm{Re}_x^{1/2}}{\theta(0,\tau)}, \tag{30}$$

$$C_{fx} = \mathrm{Re}_x^{-1/2}[\phi f''(0,\tau) + \lambda^* s'(0,\tau)], \tag{31}$$

where

$$\lambda^* = \frac{\mathrm{Gr}_x^*}{\mathrm{Re}_x^{5/2}},\quad \mathrm{Gr}_x^* = g\beta\, q_w x^4\ (k\nu^2). \tag{32}$$

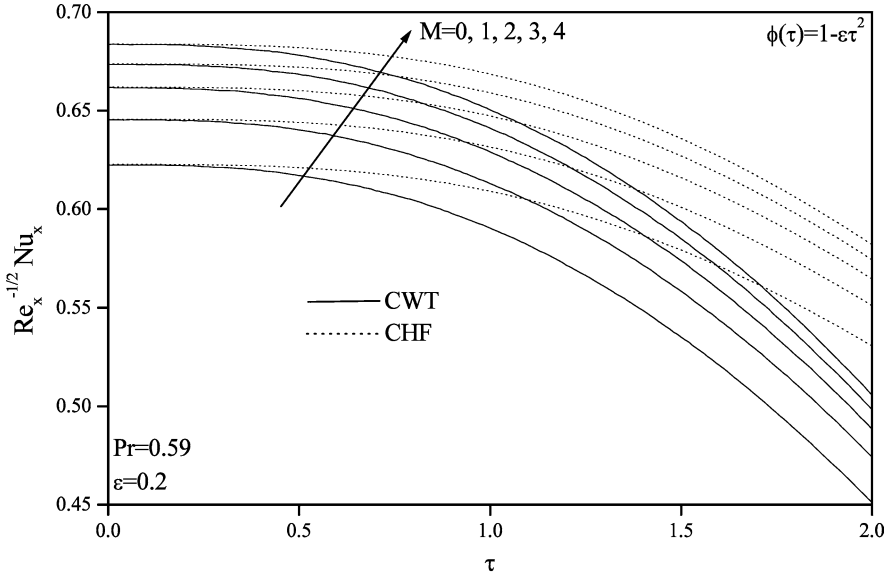

Fig. 12 Effect of magnetic parameter M on the Nusselt number, $\mathrm{Re}_x^{-1/2}\,\mathrm{Nu}_x$, for decelerating flow

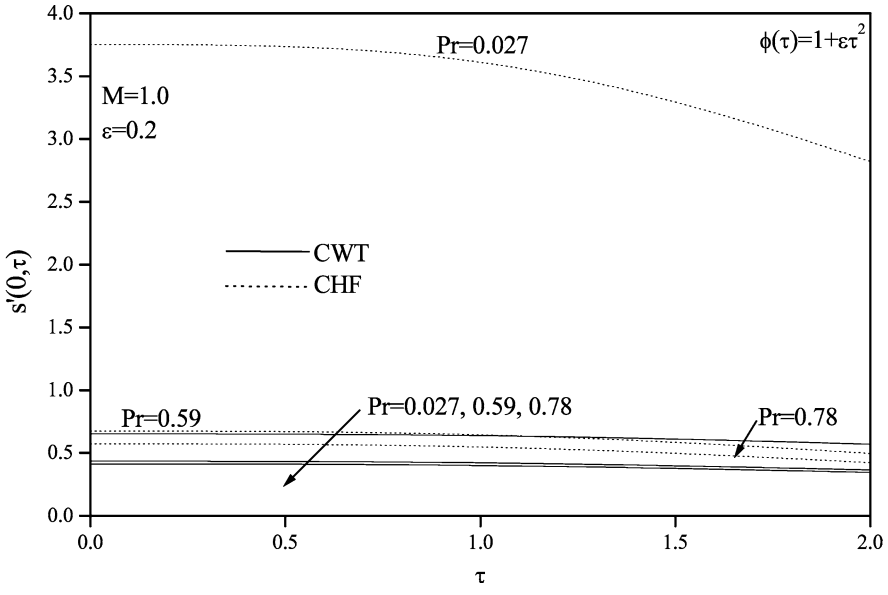

Fig. 13 Effect of the Prandtl number, Pr, on the surface shear stress in the secondary flow, $s'(0, \tau)$

Here Nu_x is the local Nusselt number, C_{fx} is the local skin friction coefficient, Re_x is the local Reynolds number, Gr_x and Gr_x^* are the local Grashof numbers for the CWT and CHF cases, respectively, λ and λ^* are the buoyancy parameters for the CWT and CHF cases, respectively, q_w is the constant heat flux at the wall, v_0 is the free stream velocity at $\tau = 0$, k is the thermal conductivity, and μ is the coefficient of viscosity.

3 Finite-difference method

The parabolic partial differential equations 14, 15, 16 under initial and boundary conditions (18) and (19) have been solved numerically by using an implicit, iterative, triagonal finite difference scheme similar to those of Blottner [25]. All the first-order derivatives with respect to τ is replaced by two-point backward difference formulae of the form

$$\frac{\partial R}{\partial \tau} = \frac{R_{i,j} - R_{i-i,j}}{\nabla \tau}, \tag{33}$$

where R is any dependent variable, and i and j are the node locations along τ and η directions, respectively. First the third-order partial differential equation 14 is converted into a second-order by substituting $f' = F$. Then the second-order partial differential equations for F, s and φ are discretized by using three-point central-differential formulae while all the first-order derivatives are discretized by employing the trapezoidal rule. At each line of constant τ, a system of algebraic equations is obtained. The function f is evaluated from the relation $f = \int_0^{\eta} F \partial \eta$. The nonlinear terms are evaluated at the previous iteration. These algebraic equations are solved

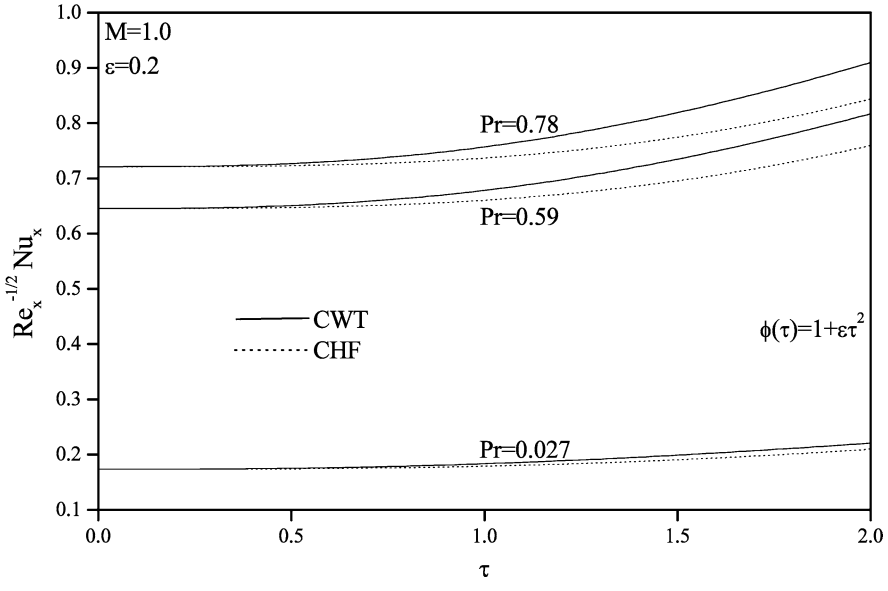

Fig. 14 Effects of Pr on the Nusselt number $Re_x^{-1/2}\ Nu_x$

iteratively by using the Thomas algorithms (see Blottner [25]). The same process is repeated for the next τ value and the problem is solved line by line until the required τ value is reached. A convergence criterion based on the relative difference between the current and previous iterations has been used. When this difference reaches 10^{-5}, the solution is assumed to have converged and the iterative process is terminated.

We have examined the effect of the grid size $\Delta\eta$ and $\Delta\tau$ and the edge of the boundary layer η_∞ on the solution. The results presented here are independent of the grid size and η_∞ at least up to three decimal place.

4 Differential-difference method

The partial differential equations 14, 15, 16 under initial and boundary conditions (18) and (19) have also been solved by using the differential-difference method [12]. In this method, we have to solve ordinary differential equations instead of partial differential equations. Further, these ordinary differential equations are converted to integral equations and then solved by an iterative numerical quadrature. The results are found to be nearly same as those obtained by the finite-difference method, but the computational time is much less.

First, we replace the derivatives with respect to τ at $\tau = \tau_I = ih$ ($i = 0, 1, 2, \ldots$), where h is a constant interval, by using four-point Gregory–Newton's formula. Equations 14, 15, 16 can be replaced by the following ordinary differential equations

$$f_i''' + 2\phi(ih) f_i f_i'' - \left[M + \phi^{-1}(ih)\left[\frac{\mathrm{d}\phi(ih)}{\mathrm{d}\tau}\right]\right](f_i' - 1) - (6h)^{-1}(11f_1' - 18f_{i-1}' + 9f_{i-2}' - 2f_{i-3}') = 0, \quad (34)$$

$$s_i'' + 2\phi(ih) f_i s_i' - (M + f_i')s_i + \theta_i - (6h)^{-1} \times (11s_i - 18s_{i-1} + 9s_{i-2} - 2s_{i-3}) = 0, \quad (35)$$

$$\theta_i'' + 2\mathrm{Pr}\,\phi(ih) f_i \theta_i' - \mathrm{Pr}(6h)^{-1}(110_i - 18\theta_{i-1} + 9\theta_{i-2} - 2\theta_{I-3}) = 0, \quad (36)$$

where

$$\theta(\tau) = 1 + \varepsilon\tau^2, \quad \frac{\mathrm{d}\phi}{\mathrm{d}\tau} = 2\varepsilon\tau, \quad \phi(ih) = 1 + \varepsilon(ih)^2, \quad \frac{\mathrm{d}\phi(ih)}{\mathrm{d}\tau} = 2\varepsilon(ih). \quad (37)$$

The boundary conditions (19) can be re-written as

$$f_i(0) = f_i'(0) = s_i(0) = \theta_I(0) - 1 = 0, \quad f_i'(\infty) - 1 = s_i(\infty) = \theta_I(\infty) = 0. \quad (38)$$

We can now express the solutions of Eqs. 34, 35, 36 with relation (37) and boundary conditions (38) at the ith station $\tau_I = ih$ in terms of the following integral equations

$$f_i' = \int_0^\eta E(\eta) \int_0^\eta \frac{G(\eta)}{E(\eta)} - \left[\int_0^\eta E(\eta) \int_0^\eta \frac{G(\eta)}{E(\eta)}\mathrm{d}\eta\,\mathrm{d}\eta\right]\frac{H(\eta)}{H(\infty)}, \quad (39)$$

$$f_i = \int_0^\eta f_i' \mathrm{d}\eta, \quad (40)$$

$$s_i = \int_0^\eta E(\eta) \int_0^\eta \frac{L(\eta)}{E(\eta)}\mathrm{d}\eta\,\mathrm{d}\eta - \left[\int_0^\eta E(\eta) \int_0^\eta \frac{L(\eta)}{E(\eta)}\mathrm{d}\eta\,\mathrm{d}\eta\right]\frac{H(\eta)}{H(\infty)}, \quad (41)$$

$$f_i' = 1 + \int_0^\eta E_1(\eta) \int_0^\eta \frac{N(\eta)}{E_1(\eta)}\mathrm{d}\eta\,\mathrm{d}\eta - \left[\int_0^\eta E_1(\eta) \int_0^\eta \frac{N(\eta)}{E_1(\eta)}\mathrm{d}\eta\,\mathrm{d}\eta\right]\frac{H_1(\eta)}{H_1(\infty)}, \quad (42)$$

where

$$E(\eta) = \mathrm{e}^{-2\phi(ih)\ f_i}, \quad H(\eta) = \int_0^\eta E(\eta)\,\mathrm{d}\eta,$$

$$G(\eta) = \left[M + \phi^{-1}(ih)\,\frac{\mathrm{d}\phi(ih)}{\mathrm{d}\tau}\right](f_i' - 1) + (6h)^{-1} \times (11f_i' - 18f_{i-1}' + 9f_{i-2}' - 2f_{i-3}'),$$

$$L(\eta) = (M + f_i')\,s_i - \theta_i + (6h)^{-1} \times (11s_i - 18s_{i-1} + 9s_{i-2} - 2s_{i-3}),$$

$$E_i(\eta) = \mathrm{e}^{-2\mathrm{Pr}\,\phi(ih)\ f_i}, \quad H_i(\eta) = \int_0^\eta E_i(\eta)\mathrm{d}\eta$$

$$N(\eta) = \mathrm{Pr}(6h)^{-1}\ (11\theta_i - 18\theta_{i-1} + 9\theta_{i-2} - 2\theta_{i-3}). \quad (43)$$

The integral equations 39, 40, 41, 42 have been solved by an iterative numerical quadrature using the Simpson's rule. Equations 39, 40, 41, 42 involved f'_i, s_i and θ_I at τ_{i-1}, τ_{i-2} and τ_{i-3}. When these equations are determined, we can get f'_i, f_i, s_i and θ_i from Eqs. 39, 40, 41, 42. The initial solutions f_0, f'_0, θ_0 at $\tau = 0$ are the solutions of the ordinary differential equations 20, 21 and 22 under boundary conditions (24), which are solved numerically by using Runge-Kutta subroutine [28]. Similarly, $f_i(\eta)$, $f'_i(\eta)$, $s_i(\eta)$ and $\theta_I(\eta)$ at $\tau = \tau_1$ and $\tau = \tau_2$ are obtained from equations similar to those of Eqs. 34, 35, 36, where the derivatives with respect to τ are, respectively, replaced by two-point and three-point difference formulae instead of four-point formula used in Eqs. 34, 35,

36. After these starting solutions have been obtained, we can solve Eqs. 39, 40, 41 and 42. The convergence criterion is based on the relative difference between the current and previous iterations. When this difference reaches 10^{-5}, the solution is assumed to have converted and the iterative process is terminated. The results are found to be in very good agreement with those of the finite difference method. The maximum difference is about 1%.

5 Results and discussion

Equations 14, 15, 16 under initial and boundary conditions (18) and (19) have been solved by using implicit finite-difference scheme and differential-difference method as described earlier. In order to assess the accuracy of our methods, we have compared the surface shear stress for the primary flow ($f''(0)$) and the surface heat transfer ($-\theta'(0)$) for the CWT case when the flow is steady with the tabulated results of Sparrow et al. [26]. The results are found to be in very good agreement. The maximum difference is found to be less than 0.5%. Hence, for the sake of brevity, the comparison is not presented here. The Nusselt number ($\mathrm{Re}_x^{-1/2}\ \mathrm{Nu}_x$) for the CWT case obtained by the differential-difference method, when $\theta(\tau)=1+\varepsilon\tau^2$, $\varepsilon=0.2$, $\mathrm{Pr}=0.7$, is compared with that obtained by the finite-difference method. The results are in very good agreement. The comparison is shown in Fig. 1.

Figures 2, 3, 4, 5 and 6 present the effect of the magnetic parameter M on the primary flow velocity, $f'(\eta, \tau)$, secondary flow velocity, $s(\eta, \tau)$, temperature, $\theta(\eta, \tau)$, and pressure $P(\eta, \tau)$, for both CWT and CHF cases when $\theta(\tau)=1+\varepsilon\tau^2$, $\varepsilon=0.2$, $\tau=1$, $\mathrm{Pr}=0.7$. Since the magnetic field exerts a stabilizing effect on the flow and temperature fields, the velocity profiles in the primary flow ($f'(\eta, \tau)$ and pressure ($P(\eta, \tau)$) increase with M, but the temperature ($\theta(\eta, \tau)$) decreases. Also the magnetic parameter M reduces the secondary flow velocity ($s(\eta, \tau)$) as is evident from Fig. 4. The secondary flow velocity, $s(\eta, \tau)$, and temperature, $\theta(\eta, \tau)$ depend strongly on the nature of the boundary conditions on the temperature θ (i.e., whether wall temperature or heat flux is constant at the wall). The velocity, $s(\eta, \tau)$ and the temperature, $\theta(\eta, \tau)$, for the CHF case are more higher than those of the CWT case. The primary flow velocity, $f'(\eta, \tau)$, and the pressure, $P(\eta, \tau)$, are independent of these conditions (see Eqs. 14 and 17).

Figures 7, 8 and 9 show the effect of the magnetic parameter M on the surface shear stresses in the primary and secondary flows ($f''(0, \tau)$, $s'(0, \tau)$) and the Nusselt number ($\mathrm{Re}_x^{-1/2}\ \mathrm{Nu}_x$) for both CWT and CHF cases when $\theta(\tau)=1+\varepsilon\tau^2$, $\varepsilon=0.2$, $\mathrm{Pr}=0.7$. The surface shear stress for the primary flow ($f''(0, \tau)$) and Nusselt number ($\mathrm{Re}_x^{-1/2}\ \mathrm{Nu}_x$) increases with M, but the surface shear stress for the secondary flow ($s'(0, \tau)$) decreases. This behavior is due to the fact that the primary flow and temperature field are accelerated by the magnetic parameter M which results in increase in velocity and temperature gradients and hence in Nusselt number. On the other hand, the magnetic parameter M reduces the secondary flow. Consequently, the secondary flow shear stress ($s'(0, \tau)$) decreases with increasing M. For the CWT case, when $\mathrm{Pr}=0.7$ and $\tau=1$. The shear stress for the primary flow ($f''(0, \tau)$) and the Nusselt number ($\mathrm{Re}_x^{-1/2}\ \mathrm{Nu}_x$) increase by 60 and 10%, respectively, as M increases from 0 to 4, whereas the secondary flow shear stress ($s'(0, \tau)$) decreases by about 33%. For a fixed M and τ, the Nusselt number for the CWT case is higher than that of the CHF case, whereas for the secondary flow shear stress ($s'(0, \tau)$) it is the other way around. Also the difference increases with time τ. Further the skin friction coefficient ($\mathrm{Re}_x^{1/2}\ C_{fx}$) for the CWT and CHF cases increase wit the buoyancy parameter λ or λ^*.

The corresponding results for the shear stresses $f''(0, \tau)$ and $s'(0, \tau)$ and the Nusselt number ($\mathrm{Re}_x^{-1/2}\ \mathrm{Nu}_x$) for decelerating free stream velocity, $\phi(\tau)=1-\varepsilon\tau^2$, $\varepsilon=0.2$, are displayed in Figs. 10, 11 and 12. The results are qualitatively similar to those of the accelerating flow ($\phi(\tau)=1+\varepsilon\tau^2$, $\varepsilon=0.2$) except that the shear stress for the primary flow ($f'(0, \tau)$) and the Nusselt number ($\mathrm{Re}_x^{-1/2}\ \mathrm{Nu}_x$) decrease with increasing time τ. However, one interesting result is that the primary flow shear stress ($f''(0, \tau)$) for $M=0$, $\tau=1.83$ vanish and beyond this value it becomes negative. This implies that there is a flow reversal in the primary flow velocity profiles ($f'(\eta, \tau)$. The magnetic field delays or prevents the flow reversal. However, the vanishing of the shear stress does not imply separation for unsteady flows [29]. The results of the decelerating flow are not the mirror reflection of the accelerating flow.

Figures 13 and 14 show the effect of the Prandtl number Pr on the surface shear stress for the secondary flow ($s'(0, \tau)$) and the Nusselt number ($\mathrm{Re}_x^{-1/2}\ \mathrm{Nu}_x$) for the CWT and CHF cases when $\varphi(\tau)=1+\varepsilon\tau^2$, $\varepsilon=0.2$, $M=1$. Since the Prandtl number Pr does not affect the shear stress for the primary flow ($f'(0, \tau)$) and the pressure ($P(\eta, \tau)$), they are not shown here. Since the thermal boundary layer becomes thinner with increasing Pr, the Nusselt number ($\mathrm{Re}_x^{-1/2}\ \mathrm{Nu}_x$) increases significantly with Pr. Further the surface shear stress in the secondary flow ($s'(0, \tau)$), which depends on the temperature θ, decreases with increasing Pr. For the CWT case, when $M=\tau=1$, the Nusselt number ($\mathrm{Re}_x^{-1/2}\ \mathrm{Nu}_x$) increases by about 200% as Pr increases from 0.7 to 15, whereas the secondary flow shear stress ($s'(0, \tau)$) decreases by about 25%.

6 Conclusions

The magnetic field increases the surface shear stress for the primary flow and the Nusselt number, but the surface shear stress for the secondary flow decreases. The Nusselt number for the constant wall temperature case is found to be higher than that of the constant heat flux case. For decelerating free stream velocity, the surface

shear stress in the primary flow vanishes at a certain instant of time and beyond this time the flow reversal occurs. The magnetic field delays or prevents the flow reversal. The Prandtl number increases the Nusselt number, but reduces the surface shear stress in the secondary flow.

References

1. Sparrow EM, Eichhorn R, Gregg JC (1959) Combined forced and free convection in a boundary layer flow. Phys Fluids 2:319–328
2. Sparrow EM, Gregg JC (1959) Buoyancy effects in forced convection flow and heat transfer. J Appl Mech 26:133–138
3. Merkin JH (1969) The effect of buoyancy forces on the boundary layer flow over a semi-infinite vertical plate in a uniform stream. J Fluid Mech 35:439–450
4. Oosthuizen PH, Hart H (1973) A numerical study of laminar combined convective flow over a flat plate. J Heat Transfer 95:60–63
5. Mucoglu A, Chen TS (1979) Mixed convection on inclined surfaces. J Heat Transfer 101:422–426
6. Cebeci T, Bradshaw P (1977) Momentum transfer in boundary layers. Hemishere Publishing Corporation, Washington
7. Sparrow EM, Lu HS (1971) Local non-similarity thermal boundary layer solutions. ASME J Heat Transfer 93:328–334
8. Merkin JH, Mahmood T (1989) Mixed convection boundary layer similarity solution: prescribed heat flux. ZAM P 40:61–68
9. Wickern G (1991) Mixed convection from an arbitrarily inclined semi-infinite flat plate-I, The influence of inclination angle. Int J Heat Mass Transfer 34:1935–1945
10. Wickern G (1991) Mixed convection from an arbitrarily inclined semi-infinite flat plate-II, The influence of the Prandtl number. Int J Heat Mass Transfer 34:1947–1957
11. Watanabe T (1991) Forced free mixed convection boundary layer flow with uniform suction or injection on a vertical flat plate. Acta Mech 89:123–132
12. Jaffe NA, Smith AMO (1972) Calculation of laminar boundary layers by means of a differential-difference method. Progress of aerospace sciences. Pergamon, New York
13. Ramachandran N, Chen TS, Armaly BF (1998) Mixed convection in stagnation flows adjacent to vertical surfaces. ASME J Heat Transfer 110:373–377
14. Nachtsheim PA, Swigert P (1965) Satisfaction of asymptotic boundary conditions in numerical solution of system of nonlinear equations of boundary layer type. NASA TN D-3004
15. Amin N, Riley N (1995) Mixed convection at a stagnation point. Q J Mech Appl Math 48:111–121
16. Brown SN, Riley N (1973) Flow past a suddenly heated vertical plate. J Fluid Mech 59:225–237
17. Ingham DB (1985) Flow past a suddenly heated vertical plate. Proc R Soc A402:109–134
18. Sammakia B, Gebhart B, Carey VP (1982) Transient mixed convection adjacent to a vertical flat plate. Int J Heat Mass Transfer 25:835–846
19. Harris SD, Elliott L, Ingham DB, Pop I (1998) Transient free convection flow past a vertical flat plate subject to a sudden change in surface temperature. Int J Mass Transfer 41:357–372
20. Sashadri R, Sreeshylan N, Nath G (2002) Unsteady mixed convection flow in the stagnation region of a heated vertical plate due to impulsive motion. Int J Heat Mass Transfer 45:1345–1352
21. Wang CY (1987) Effect of natural convection on the axisymmetric stagnation-point flow on a vertical plate. J Appl Mech 54:724–726
22. Rott N, Lewellen W (1967) Boundary layers due to the combined effects of rotation and translation. Phys Fluids 10:1867–1873
23. Chawla SS, Verma AR (1983) Free convection from a disk rotating in a vertical plane. J Fluid Mech 126:307–313
24. Thacker WT, Watson LT, Kumar SK (1990) Magnetohydrodynamic free convection from a disk rotatign in a vertical plane. Appl Math Modelling 14:527–537
25. Blottner FG (1970) Finite-difference method of solution of the boundary layer equations. AIAA J 8:193–205
26. Sparrow EM, Eckert ERG, Minkowycz WJ (1962) Transpiration cooling in a magnetohydrodynamic stagnation-point flow. Appl Sci Res A11:125–152
27. Eringen AC, Maugin GA (1990) Electrodynamics of continua, vol II. Springer, Berlin Heidelberg New York
28. Na TY (1979) Computational methods in engineering boundary value problems. Academic, New York
29. Smith FT (1986) Steady and unsteady boundary layer separation. Ann Rev Fluid Mech 18:197–220